Hindawi
Mathematical Problems in Engineering
Volume 2017, Article ID 5093404, 10 pages
https://doi.org/10.1155/2017/5093404

Research Article

Thermoelastic Analysis for Two Collinear Cracks in an Orthotropic Solid Disturbed by Antisymmetrical Linear Heat Flow

Bing Wu,[1,2,3] Jun-gao Zhu,[1,2] Daren Peng,[3] Rhys Jones,[3] Shi-hu Gao,[1,2] and Yang-yang Lu[1,2]

[1]*Key Laboratory of Ministry of Education for Geomechanics and Embankment Engineering, Hohai University, Nanjing, Jiangsu 210098, China*
[2]*Jiangsu Research Center of Geotechnical Engineering Technology, Hohai University, Nanjing, Jiangsu 210098, China*
[3]*Department of Mechanical and Aerospace Engineering, Monash University, Clayton, VIC 3800, Australia*

Correspondence should be addressed to Jun-gao Zhu; 2841453079@qq.com

Received 2 May 2017; Revised 19 July 2017; Accepted 31 July 2017; Published 19 November 2017

Academic Editor: Nunzio Salerno

The problem of two collinear cracks in an orthotropic solid under antisymmetrical linear heat flow is investigated. It is assumed that there exists thermal resistance to heat conduction through the crack region. Applying the Fourier transform, the thermal coupling partial differential equations are transformed to dual integral equations and then to singular integral equations. The crack-tip thermoelastic fields including the jumps of temperature and elastic displacements on the cracks and the mode II stress intensity factors are obtained explicitly. Numerical results show the effects of the geometries of the cracks and the dimensionless thermal resistance on the temperature change and the mode II stress intensity factors. Also, FEM solutions for the stress intensity factor K are used to compare with the solutions obtained using the method. It is revealed that the friction in closed crack surface region should be considered in analyzing the stress intensity factor K.

1. Introduction

In engineering problems, the thermoelastic analysis for a cracked material has attracted much interest [1–5]. The thermal stress analysis for a cracked isotropic or anisotropic material has attracted much attention. A large number of related papers have been published to address fracture behaviors of isotropic and anisotropic solid. For example, the singularity of the stress fields near the crack-tip with a specified temperature or heat flux loading is studied by Sih [6]. The stress intensity factors of a central crack in an orthotropic material under a uniform heat flow are given by Tsai [7]. The thermoelasticity problem of two collinear cracks embedded in an orthotropic solid has been considered by Chen and Zhang [8]. By using the J-integral obtained from the finite element solutions, the stress intensity factor has been computed by Wilson and Yu [9]. Two alternative approaches for analyzing the nonlinear interaction between two equal-length collinear cracks subjected to remote tensile stress on infinity are developed by Chang and Kotousov [10]. By using a two-dimensional dual boundary element method, the stress intensity factors of a cracked isotropic material under the transient thermoelastic loadings have been calculated by Prasad et al. [11]. The diffraction of plane temperature-step waves by a crack in an orthotropic thermoelastic solid has been investigated by Brock [12]. The steady-state thermoelasticity problem of a cracked fiber-reinforced slab under a state of generalized plane deformation is studied [13]. Using the hyperbolic heat conduction theory and the dual-phase-lag heat conduction model, the transient temperature and thermal stresses around a partially insulated crack in a thermoelastic strip under a temperature impact and the transient temperature field around a partially insulated crack in a half plane are obtained by Hu and Chen [14, 15]. The thermal-medium crack model proposed by Zhong and Lee [16] is applied to investigate the problem of a penny-shaped crack in an infinite isotropic material [17]. Development of a unified model for the steady-state

operation of single-phase natural circulation loops is made by Basu et al. [18]. An unsymmetrical end-notched flexure test is described and its suitability for interfacial fracture toughness testing is evaluated [19]. An infinite functionally graded medium with a partially insulated crack subjected to a steady-state heat flux away from the crack region as well as mechanical crack surface stresses is considered [20]. The influence of an axisymmetric partially insulated mixed-mode crack on the coupled response of a functionally graded magnetoelectroelastic material subjected to thermal loading is investigated [21]. The elastic-static problem of a partially insulated axisymmetric crack embedded in a graded coating bonded to a homogeneous substrate subjected to thermal loading is considered [22]. In order to investigate the crack problems in elastic material, many mathematical methods have been widely used such as the integral equation method [23], the linear sampling method [24], and the Trefftz method [25].

In the abovementioned works and other works [26–32], the partially insulated boundary condition is mainly used and the closed-form solutions have been obtained for the thermoelastic field around the penny-shaped crack under the loading of uniform heat flow.

Under the consideration of the antisymmetrical linear heat flow, the partially insulated boundary condition is applied to address the problem of two collinear cracks in an orthotropic solid and FEM solutions for the stress intensity factor K are used to investigate the accuracy of this methodology in this paper. Applying the Fourier transform technique and integral equation methods, the crack-tip thermoelastic fields involving the jumps of temperature, the elastic displacements across the cracks, and the mode II stress intensity factors are given in explicit forms. Numerical results show the heat flux to the crack surfaces and the mode II stress intensity factors are dependent on the geometries of cracks and the dimensionless thermal resistance. The thermal resistance in the heat conduction through the crack region is of much importance in analyzing the thermoelastic problem of a cracked material with a thermal loading. Furthermore, FEM solutions for the stress intensity factor K are used to compare with the solutions obtained using the method. It is revealed the friction in closed crack surface region has an effect on analyzing the stress intensity factor K and should be considered.

2. Statement of the Problem

As shown in Figure 1, two collinear cracks for an infinite transversely orthotropic material are embedded in an orthotropic solid. We use Cartesian coordinates system xoy and suppose that the two collinear cracks are situated at the segment of $|a| < |x| < |b|$. With respect to the state of plane stress, the following constitute equations are

$$\sigma_{xx} = c_{11}\frac{\partial u}{\partial x} + c_{12}\frac{\partial v}{\partial y} - \beta_1\theta,$$

$$\sigma_{yy} = c_{12}\frac{\partial u}{\partial x} + c_{22}\frac{\partial v}{\partial y} - \beta_2\theta,$$

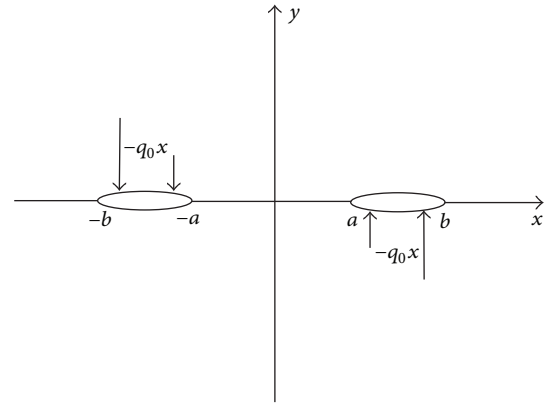

Figure 1: Two collinear cracks in an orthotropic material under antisymmetrical linear heat flow.

$$\sigma_{xy} = c_{66}\left[\frac{\partial u}{\partial y} + \frac{\partial v}{\partial x}\right],$$

$$c_{11} = \frac{E_{xx}}{1 - \nu_{xy}\nu_{yx}},$$

$$c_{22} = \frac{E_{yy}}{1 - \nu_{xy}\nu_{yx}},$$

$$c_{12} = \frac{E_{xx}\nu_{yx}}{1 - \nu_{xy}\nu_{yx}} = \frac{E_{yy}\nu_{xy}}{1 - \nu_{xy}\nu_{yx}},$$

$$\beta_1 = c_{11}\alpha_{xx} + c_{12}\alpha_{yy},$$

$$\beta_2 = c_{12}\alpha_{xx} + c_{22}\alpha_{yy}, \tag{1}$$

where u and v denote the components of elastic displacement, θ stands for the temperature change, ν_{xy} and ν_{yx} are the Poisson ratios, E_{xx} and E_{yy} are Young's moduli, $c_{66} = G_{xy}$ is the shear modulus, and α_{xx} and α_{yy} are the coefficients of linear expansion. Applying the following equations:

$$\frac{\partial \sigma_{xx}}{\partial x} + \frac{\partial \sigma_{yy}}{\partial y} = 0,$$

$$\frac{\partial \sigma_{xy}}{\partial x} + \frac{\partial \sigma_{yy}}{\partial y} = 0, \tag{2}$$

we have

$$c_{11}\frac{\partial^2 u}{\partial x^2} + c_{66}\frac{\partial^2 u}{\partial y^2} + (c_{12} + c_{66})\frac{\partial^2 v}{\partial x \partial y} - \beta_1\frac{\partial \theta}{\partial x} = 0,$$

$$c_{66}\frac{\partial^2 v}{\partial x^2} + c_{22}\frac{\partial^2 v}{\partial y^2} + (c_{12} + c_{66})\frac{\partial^2 u}{\partial x \partial y} - \beta_2\frac{\partial \theta}{\partial y} = 0. \tag{3}$$

Furthermore, applying thermal equilibrium equation leads to

$$\lambda^2\frac{\partial^2 \theta}{\partial x^2} + \frac{\partial^2 \theta}{\partial y^2} = 0, \quad \lambda = \sqrt{\frac{\lambda_x}{\lambda_y}}, \tag{4}$$

where λ_x and λ_y are the thermal conductivities of a cracked orthotropic material. From the theory of Fourier heat conduction, one has

$$q_x = -\lambda_x \frac{\partial \theta}{\partial x}, \qquad q_y = -\lambda_y \frac{\partial \theta}{\partial y}. \tag{5}$$

Due to the antisymmetry of the heat flux acting on two collinear cracks, the thermal field in the region $x > 0$ is only studied. With application of the crack-face boundary conditions, one has

$$\sigma_{yy}^{+}(x,0) = \sigma_{yy}^{-}(x,0) = 0, \quad \sigma_{xy}^{+}(x,0) = \sigma_{xy}^{-}(x,0) = 0, \quad a < x < b. \tag{6}$$

For the thermal loading, the antisymmetrical linear heat flow is acting on the crack surfaces; namely,

$$q_y^{+}(x,0) = q_y^{-}(x,0) = -q_0 x, \quad a < x < b, \tag{7}$$

where q_0 is the prescribed constant, where

$$q_y^{+}(x,0) = -\lambda_y \frac{\partial \theta^{+}(x,0)}{\partial y}, \qquad q_y^{-}(x,0) = -\lambda_y \frac{\partial \theta^{-}(x,0)}{\partial y}. \tag{8}$$

Considering the thermal resistance R_c in the heat conduction through the crack region, the thermoelastic boundary conditions on the crack surfaces are written as

$$q_y^{+}(x,0) = q_y^{-}(x,0) = -\left(q_0 - q_c\right) x, \quad a < x < b, \tag{9}$$

where

$$q_c = \frac{1}{R_c}\left(\theta^{+}(x,0) - \theta^{-}(x,0)\right). \tag{10}$$

q_c denotes the heat flux to the crack surfaces. The limiting value $R_c \to 0$ or $R_c \to \infty$ represents perfect conduction or perfect insulation on the crack surfaces. In addition, the continuity of elastic displacement and temperature on the crack-free parts of x-axis yields

$$v^{+}(x,0) = v^{-}(x,0), \quad 0 < x < a, \ x > b, \tag{11}$$

$$u^{+}(x,0) = u^{-}(x,0), \quad 0 < x < a, \ x > b, \tag{12}$$

$$\theta^{+}(x,0) = \theta^{-}(x,0), \quad q_y^{+}(x,0) = q_y^{-}(x,0), \quad 0 < x < a, \ x > b. \tag{13}$$

3. Solution Procedure

3.1. Temperature Field. The temperature field is not dependent on the elastic strain; the temperature field can be solved firstly. By applying the Fourier transform technique, the solution of (4) can be defined as

$$\theta^{\pm}(x,y) = \int_0^{\infty} A^{\pm}(\xi)\, e^{-\xi\delta^{\pm}\lambda y} \sin(\xi x)\, d\xi. \tag{14}$$

$A^{\pm}(\xi)$ is unknown and will be solved. $\delta^{+} = 1$ for $y > 0$ and $\delta^{-} = -1$ for $y < 0$. Hereafter the superscripts + and − denote the physical quantities of the upper (i.e., $y > 0$) and lower (i.e., $y < 0$) region, respectively. From (5), we obtain

$$q_x^{\pm}(x,y) = -\lambda_x \int_0^{\infty} \xi A^{\pm}(\xi)\, e^{-\xi\delta^{\pm}\lambda y} \cos(\xi x)\, d\xi, \qquad q_y^{\pm}(x,y) = \lambda\lambda_y \delta^{\pm} \int_0^{\infty} \xi A^{\pm}(\xi)\, e^{-\xi\delta^{\pm}\lambda y} \sin(\xi x)\, d\xi. \tag{15}$$

Using (8) and the second relation in (13), we obtain

$$A^{+}(\xi) = -A^{-}(\xi). \tag{16}$$

Using the boundary conditions (7), one has

$$\int_0^{\infty} \xi A^{+}(\xi) \sin(\xi x)\, d\xi = -\frac{\left(q_0 - q_c\right) x}{\lambda\lambda_y}, \quad a < x < b. \tag{17}$$

Application of the first relation in (13) leads to

$$\int_0^{\infty} A^{+}(\xi) \sin(\xi x)\, d\xi = 0, \quad 0 < x < a \text{ or } x > b. \tag{18}$$

In order to solve (17) and (18), we give a definition of the auxiliary function

$$\omega(x) = \frac{\partial \theta^{+}(x,0)}{\partial x}. \tag{19}$$

Applying the inverse Fourier transform, one obtains

$$A^{+}(\xi)\,\xi = \frac{2}{\pi}\int_a^b \omega(s) \cos(\xi s)\, ds. \tag{20}$$

Substituting (20) into (17) leads to

$$\frac{2}{\pi}\int_a^b \omega(s)\, ds \int_0^{\infty} \sin(\xi x)\cos(\xi s)\, d\xi = -\frac{\left(q_0 - q_c\right) x}{\lambda\lambda_y}, \quad a < x < b. \tag{21}$$

From the known result [33]

$$2\int_0^{\infty} \sin(\xi x)\cos(\xi s)\, d\xi = \frac{1}{x+s} + \frac{1}{x-s}. \tag{22}$$

Equation (21) can be rewritten as

$$\frac{1}{\pi}\int_a^b \omega(s)\, \frac{2}{s^2 - x^2}\, ds = \frac{q_0 - q_c}{\lambda\lambda_y}, \quad a < x < b. \tag{23}$$

Then, introducing $s^2 = s^*$, $x^2 = x^*$, $2s\,ds = ds^*$, $a^2 = a^*$, and $b^2 = b^*$, (23) can be written as

$$\frac{1}{\pi}\int_{a^*}^{b^*}\omega^*(s^*)\frac{1}{(s^*-x^*)\sqrt{s^*}}ds^* = \frac{q_0-q_c}{\lambda\lambda_y}, \quad a<x<b. \tag{24}$$

By virtue of the singular integral equation theory, we can obtain the solution of (21); namely,

$$\frac{\omega^*(x^*)}{\sqrt{x^*}} = \frac{1}{\pi\sqrt{(x^*-a^*)(b^*-x^*)}} \cdot\int_{a^*}^{b^*}\frac{\sqrt{(s^*-a^*)(b^*-s^*)}}{x^*-s^*}\frac{q_0-q_c}{\lambda\lambda_y}ds^* + \frac{C}{\sqrt{(x^*-a^*)(b^*-x^*)}}, \tag{25}$$

where C is the constant determined by

$$\frac{1}{2}\int_{a^*}^{b^*}\frac{\omega^*(s^*)}{\sqrt{s^*}}ds^* = 0. \tag{26}$$

By some computations, we can get $C = 0$. Furthermore, applying (19) and (25) yields

$$\theta^+(x,0) = \int_{a^*}^{x^*}\frac{\omega^*(s^*)}{2\sqrt{s^*}}ds^*. \tag{27}$$

Substituting (25) into (27), we get the temperature change on the cracks as

$$\theta^+(x,0) = -\frac{q_0-q_c}{\lambda\lambda_y(b^2-a^2)}\sqrt{(x^2-a^2)(b^2-x^2)}, \quad a<x<b. \tag{28}$$

When $a = 0$, the temperature change on the cracks of a single crack of length $2b$ is given as

$$\theta^+(x,0) = -\frac{(q_0-q_c)x}{\lambda\lambda_y b^2}\sqrt{b^2-x^2}, \quad 0<x<b. \tag{29}$$

3.2. Elastic Field. In what follows, we pay an attention to the solutions of the partial differential equations (3). $u^\pm(x,y)$ and $v^\pm(x,y)$ are written as two parts

$$u^\pm(x,y) = u_1^\pm(x,y) + u_2^\pm(x,y), \qquad v^\pm(x,y) = v_1^\pm(x,y) + v_2^\pm(x,y). \tag{30}$$

$u_1^\pm(x,y)$ and $v_1^\pm(x,y)$ correspond to the general solutions under $\theta^\pm(x,y) = 0$. $u_2^\pm(x,y)$ and $v_2^\pm(x,y)$ are the particular solutions under a thermal flux loading. With application of the Fourier transform, $u_1^\pm(x,y)$ and $v_1^\pm(x,y)$ can be expressed as

$$u_1^\pm(x,y) = \sum_{j=1}^{2}\int_0^\infty A_j^\pm(\xi)e^{-\xi\delta^\pm\gamma_j y}\cos(\xi x)\,d\xi, \qquad v_1^\pm(x,y) = \sum_{j=1}^{2}\int_0^\infty \eta_j\delta^\mp A_j^\pm(\xi)e^{-\xi\delta^\pm\gamma_j y}\sin(\xi x)\,d\xi. \tag{31}$$

$A_j^\pm(\xi)$ $(j = 1,2)$ are unknown to be solved. γ_j $(j = 1,2)$ are the roots of equation as follows: $(\mathrm{Re}\,\gamma(j) > 0)$

$$c_{22}c_{66}\gamma^4 + \left(c_{12}^2 + 2c_{12}c_{66} - c_{12}c_{22}\right)\gamma^2 + c_{11}c_{66} = 0, \tag{32}$$

where η_j $(j = 1,2)$ can be calculated as follows:

$$\eta_j = \frac{c_{11}-c_{66}\gamma_j^2}{(c_{12}+c_{66})\gamma_j}. \tag{33}$$

In addition, $u_2^\pm(x,y)$ and $v_2^\pm(x,y)$ are chosen as

$$u_2^\pm(x,y) = \int_0^\infty A_*^\pm(\xi)e^{-\xi\delta^\pm\lambda y}\cos(\xi x)\,d\xi, \qquad v_2^\pm(x,y) = \int_0^\infty \delta^\mp B_*^\pm(\xi)e^{-\xi\delta^\pm\lambda y}\sin(\xi x)\,d\xi. \tag{34}$$

Substituting (34) into (3) leads to

$$\begin{bmatrix}A_*^\pm(\xi)\\ B_*^\pm(\xi)\end{bmatrix} = \frac{A^\pm(\xi)}{\xi}\begin{bmatrix}M_1\\ M_2\end{bmatrix}, \qquad \begin{bmatrix}\beta_1\\ \beta_2\lambda\end{bmatrix} = \begin{bmatrix}c_{11}-c_{66}\lambda^2 & -(c_{12}+c_{66})\lambda\\ (c_{11}+c_{66})\lambda & c_{66}-c_{22}\lambda^2\end{bmatrix}\begin{bmatrix}M_1\\ M_2\end{bmatrix}. \tag{35}$$

From (31) and (34), the components of stress can be written as

$$\sigma_{xx}^\pm(x,y) = -\sum_{j=1}^{2}\int_0^\infty\left(c_{11}-c_{12}\gamma_j\eta_j\right)\xi A_j^\pm(\xi)e^{-\xi\delta^\pm\gamma_j y}\cdot\sin(\xi x)\,d\xi - (c_{11}M_1 - c_{22}\lambda M_2 - \beta_1)\cdot\int_0^\infty A^\pm(\xi)e^{-\xi\delta^\pm\lambda y}\sin(\xi x)\,d\xi, \tag{36}$$

$$\sigma_{yy}^\pm(x,y) = -\sum_{j=1}^{2}\int_0^\infty\left(c_{12}-c_{22}\gamma_j\eta_j\right)\xi A_j^\pm(\xi)e^{-\xi\delta^\pm\gamma_j y}\cdot\sin(\xi x)\,d\xi - (c_{12}M_1 - c_{22}\lambda M_2 - \beta_2)\cdot\int_0^\infty A^\pm(\xi)e^{-\xi\delta^\pm\lambda y}\sin(\xi x)\,d\xi, \tag{37}$$

$$\sigma_{xy}^\pm(x,y) = -c_{66}\sum_{j=1}^{2}\int_0^\infty\delta^\pm\left(\gamma_j+\eta_j\right)\xi A_j^\pm(\xi)e^{-\xi\delta^\pm\gamma_j y}\cdot\cos(\xi x)\,d\xi - c_{66}\int_0^\infty\delta^\pm\left(M_1\lambda + M_2\right)A^\pm(\xi)\cdot e^{-\xi\delta^\pm\lambda y}\cos(\xi x)\,d\xi. \tag{38}$$

It is seen that the elastic field was only induced by the loading $-q_0x$. We only consider the antisymmetrical linear heat flow $-q_0x$ in this paper, and it follows that

$$\sigma_{yy}^\pm(x,0) = 0, \quad x>0. \tag{39}$$

From (37) and (39), one arrives at

$$\sum_{j=1}^{2}\left(c_{12}-c_{22}\gamma_j\eta_j\right)A_j^+(\xi) = \left(c_{22}\lambda M_2+\beta_2-c_{12}M_1\right)\frac{A^+(\xi)}{\xi}. \tag{40}$$

Utilizing the second relation of (6) and (12) yields

$$\int_0^\infty\left[\sum_{j=1}^{2}A_j^+(\xi)+\frac{M_1A^+(\xi)}{\xi}\right]\cos(\xi x)\,d\xi = 0, \quad 0<x<a,\ x>b, \tag{41}$$

$$\sum_{j=1}^{2}\int_0^\infty\left(\gamma_j+\eta_j\right)\xi A_j^+(\xi)\cos(\xi x)\,d\xi + \int_0^\infty\left(M_1\lambda+M_2\right)\xi A^+(\xi)\cos(\xi x)\,d\xi = 0, \quad a<x<b. \tag{42}$$

To solve the dual integral equations, we introduce a new auxiliary function $\varphi(x)$.

$$\varphi(x) = \frac{\partial\left[u^+(x,0)-u^-(x,0)\right]}{\partial x}. \tag{43}$$

By virtue of theory of the inverse Fourier transform, one gets

$$\sum_{j=1}^{2}A_j^+(\xi)\,\xi+M_1A^+(\xi) = -\frac{2}{\pi}\int_a^b\varphi(s)\sin(\xi s)\,ds. \tag{44}$$

Making use of (40) and (44) yields

$$\begin{aligned}A_1^+(\xi)\,\xi &= \frac{c_{22}\lambda M_2+\beta_2-c_{22}\gamma_2\eta_2M_1}{c_{22}\left(\gamma_2\eta_2-\gamma_1\eta_1\right)}A^+(\xi) + \frac{c_{12}-c_{22}\gamma_2\eta_2}{c_{22}\left(\gamma_2\eta_2-\gamma_1\eta_1\right)}\frac{2}{\pi}\int_a^b\varphi(s)\sin(\xi s)\,ds,\\ A_2^+(\xi)\,\xi &= \frac{c_{22}\gamma_1\eta_1M_1-c_{22}\lambda M_2-\beta_2}{c_{22}\left(\gamma_2\eta_2-\gamma_1\eta_1\right)}A^+(\xi) + \frac{c_{22}\gamma_1\eta_1-c_{12}}{c_{22}\left(\gamma_2\eta_2-\gamma_1\eta_1\right)}\frac{2}{\pi}\int_a^b\varphi(s)\sin(\xi s)\,ds.\end{aligned} \tag{45}$$

Application of (42) and (45) leads to

$$\frac{2}{\pi}\int_a^b\varphi(s)\,ds\int_0^\infty\cos(\xi x)\sin(\xi s)\,d\xi = K\int_0^\infty A^+(\xi)\cos(\xi x)\,d\xi, \quad a<x<b, \tag{46}$$

with

$$\begin{aligned}N_1 &= \left(\gamma_1+\eta_1\right)\left(c_{22}\gamma_2\eta_2M_1-c_{22}\lambda M_2-\beta_2\right) + \left(\gamma_2+\eta_2\right)\left(c_{22}\lambda M_2+\beta_2-c_{22}\gamma_1\eta_1M_1\right) + c_{22}\left(M_1\lambda+M_2\right)\left(\gamma_2\eta_2-\gamma_1\eta_1\right),\\ N_2 &= \left(\gamma_1+\eta_1\right)\left(c_{12}-c_{22}\gamma_2\eta_2\right) + \left(\gamma_2+\eta_2\right)\left(c_{22}\gamma_1\eta_1-c_{12}\right),\\ K &= \frac{N_1}{N_2}.\end{aligned} \tag{47}$$

With application of the inverse Fourier transform and (28), one obtains

$$K\int_0^\infty A^+(\xi)\cos(\xi x)\,d\xi = \frac{2K}{\pi}\int_a^b\theta^+(s,0)\,ds\int_0^\infty\sin(\xi s)\cos(\xi x)\,d\xi. \tag{48}$$

Recalling the known result [34]

$$\int_a^b\frac{\sqrt{(s-a)(b-s)}}{x-s}ds = \frac{\pi}{2}(2x-a-b). \tag{49}$$

Inserting (28) into (48), one gets

$$\begin{aligned}K\int_0^\infty A^+(\xi)\cos(\xi x)\,d\xi &= \frac{2K\left(q_0-q_c\right)}{\pi\lambda\lambda_y\left(b^2-a^2\right)}\int_a^b\frac{\sqrt{\left(b^2-s^2\right)\left(s^2-a^2\right)}}{x^2-s^2}2s\,ds\\ &= p\left(2x^2-a^2-b^2\right),\end{aligned} \tag{50}$$

where

$$p = \frac{K\left(q_0-q_c\right)}{\lambda\lambda_y\left(b^2-a^2\right)}. \tag{51}$$

From (46) and (50), we can get

$$\varphi^*(x^*) = \frac{1}{\pi\sqrt{(x^*-a^*)(b^*-x^*)}}\cdot\int_{a^*}^{b^*}\frac{\sqrt{(s^*-a^*)(b^*-s^*)}}{x^*-s^*}\left(2s^*-a^*-b^*\right)p\,ds^* + \frac{C}{\sqrt{(x^*-a^*)(b^*-x^*)}}, \tag{52}$$

Considering the following condition:

$$\int_{a^*}^{b^*}\frac{\varphi^*(s^*)}{2\sqrt{s^*}}ds^* = 0. \tag{53}$$

By further calculations, one obtains

$$C = -\frac{p\left(a^2-b^2\right)^2}{4} + \frac{2pb^2\left(a^2+b^2\right)E(k)}{3F(k)} - \frac{4pa^2b^2}{3}. \tag{54}$$

With application of (43), one has

$$u^+(x,0) - u^-(x,0) = \int_a^x \varphi(s)\,ds = \int_{a^*}^{x^*} \frac{\varphi^*(s^*)}{2\sqrt{s^*}}ds^*. \tag{55}$$

Substituting (52) into (55), we have

$$\begin{aligned} &u^+(x,0) - u^-(x,0) \\ &= -\frac{2}{3}p\left[b^2\left(a^2+b^2\right)\left(E(\alpha) - \frac{E(k)}{F(k)}F(\alpha)\right)\right] \\ &\quad + \frac{2}{3}px\sqrt{\left(x^2-a^2\right)\left(b^2-x^2\right)}, \quad a < x < b, \end{aligned} \tag{56}$$

where $k = \sqrt{(b^2-a^2)/b^2}$ and $F(\cdot)$ and $E(\cdot)$ are the complete elliptic integrals of the first and second kind, respectively. $F(\alpha,k)$ and $E(\alpha,k)$ are the incomplete elliptic integrals of the first and the second kinds with

$$\alpha = \arcsin\sqrt{\frac{b^2-x^2}{b^2-a^2}}. \tag{57}$$

Applying (38) and (45), the shearing stresses near the crack-tips are expressed as

$$\begin{aligned} &\sigma_{xy}^{\pm}(x,0) \\ &= \frac{c_{66}N_2}{\pi c_{22}\left(\gamma_2\eta_2-\gamma_1\eta_1\right)}\int_a^b \frac{2s\varphi(s)}{s^2-x^2}ds \\ &\quad + \frac{c_{66}N_1}{c_{22}\left(\gamma_2\eta_2-\gamma_1\eta_1\right)}\int_0^\infty A^+(\xi)\cos(\xi x)\,d\xi. \end{aligned} \tag{58}$$

Substituting (50) and (52) into (58), one has

$$\begin{aligned} \sigma_{xy}^{\pm}(x,0) &= \frac{c_{66}pN_2}{c_{22}\left(\gamma_2\eta_2-\gamma_1\eta_1\right)}\left(\frac{4a^2b^2}{3} + \frac{\left(b^2-a^2\right)^2}{2}\right. \\ &\quad \left. - \frac{2b^2\left(a^2+b^2\right)E(k)}{3F(k)} - \left(2x^2-a^2-b^2\right)^2\right) \\ &\quad \times \frac{1}{2\sqrt{\left(a^2-x^2\right)\left(b^2-x^2\right)}} \\ &\quad + \frac{c_{66}p}{2c_{22}\left(\gamma_2\eta_2-\gamma_1\eta_1\right)}\left(4N_2+N_1\right)\left(2x^2-a^2-b^2\right) \\ &\quad 0 < x < a, \end{aligned}$$

$$\begin{aligned} \sigma_{xy}^{\pm}(x,0) &= -\frac{c_{66}pN_2}{c_{22}\left(\gamma_2\eta_2-\gamma_1\eta_1\right)}\left(\frac{4a^2b^2}{3} + \frac{\left(b^2-a^2\right)^2}{2}\right. \\ &\quad \left. - \frac{2b^2\left(a^2+b^2\right)E(k)}{3F(k)} - \left(2x^2-a^2-b^2\right)^2\right) \\ &\quad \times \frac{1}{2\sqrt{\left(x^2-a^2\right)\left(x^2-b^2\right)}} \\ &\quad + \frac{c_{66}p}{2c_{22}\left(\gamma_2\eta_2-\gamma_1\eta_1\right)}\left(4N_2+N_1\right)\left(2x^2-a^2-b^2\right) \\ &\quad x > b. \end{aligned} \tag{59}$$

3.3. Stress Intensity Factors. According to (10), (16), and (28), one has

$$q_c = \frac{2h_c q_0\sqrt{\left(x^2-a^2\right)\left(b^2-x^2\right)}}{2h_c\sqrt{\left(x^2-a^2\right)\left(b^2-x^2\right)} + \lambda\lambda_y\left(b^2-a^2\right)}. \tag{60}$$

The quantity $h_c = \lambda_y/R_c$ is the dimensionless thermal resistance. One can see from (60) that the heat flux to the crack surfaces is dependent on the geometries of the cracks, the material properties, and applied thermal loading. Furthermore, the crack opening displacement has great influences on analyzing the thermoelastic problem. From the obtained results, it is easy to determine

$$\begin{aligned} \Delta u(x,0) &= u^+(x,0) - u^-(x,0), \\ K_{\mathrm{SHD}}^{\mathrm{inn}} &= \lim_{x\to a^+}\sqrt{\frac{\pi}{2(x-a)}}\Delta u(x,0), \\ K_{\mathrm{SHD}}^{\mathrm{out}} &= \lim_{x\to b^-}\sqrt{\frac{\pi}{2(b-x)}}\Delta u(x,0). \end{aligned} \tag{61}$$

From (56), one arrives at

$$\begin{aligned} K_{\mathrm{SHD}}^{\mathrm{inn}} &= -\frac{2pb^2\left(a^2+b^2\right)}{3}\left[\frac{bE(k)}{aF(k)} - \frac{a}{b}\right]\sqrt{\frac{\pi a}{\left(b^2-a^2\right)}} \\ &\quad + \frac{2pa}{3}\sqrt{\pi a\left(b^2-a^2\right)}, \\ K_{\mathrm{SHD}}^{\mathrm{out}} &= \frac{2pb^2\left(a^2+b^2\right)}{3}\left[\frac{E(k)}{F(k)} - 1\right]\sqrt{\frac{\pi b}{\left(b^2-a^2\right)}} \\ &\quad + \frac{2pb}{3}\sqrt{\pi b\left(b^2-a^2\right)}. \end{aligned} \tag{62}$$

From (62), it is seen that the stress intensity factors are expressed in the closed forms. In addition, to consider the

stress fields near the crack-tips, the mode II stress intensity factors are defined as

$$K^{\text{inn}} = \lim_{x\to a^-} \sqrt{2\pi\,(a-x)}\,\sigma_{xy}^{\pm}(x,0)\,,$$
$$K^{\text{out}} = \lim_{x\to b^+} \sqrt{2\pi\,(x-b)}\,\sigma_{xy}^{\pm}(x,0)\,. \tag{63}$$

One has

$$K^{\text{inn}} = \frac{c_{66}pN_2}{2c_{22}\left(\gamma_2\eta_2-\gamma_1\eta_1\right)}\left(\frac{4a^2b^2}{3}-\frac{\left(a^2-b^2\right)^2}{2}-\frac{2b^2\left(a^2+b^2\right)E(k)}{3F(k)}\right)\times\sqrt{\frac{\pi}{a\left(b^2-a^2\right)}},$$
$$K^{\text{out}} = -\frac{c_{66}pN_2}{2c_{22}\left(\gamma_2\eta_2-\gamma_1\eta_1\right)}\left(\frac{4a^2b^2}{3}-\frac{\left(b^2-a^2\right)^2}{2}-\frac{2b^2\left(a^2+b^2\right)E(k)}{3F(k)}\right)\times\sqrt{\frac{\pi}{b\left(b^2-a^2\right)}}. \tag{64}$$

It is easy to find that the mode II stress intensity factors are dependent not only on the geometries of the cracks and the heat flux to the crack surfaces q_c but also on the material properties.

In order to verify (64), we consider a limiting case as $a \to 0$, corresponding a single crack with the length of $2b$. It is not difficult to find

$$K_0 = \frac{c_{66}p'N_2b^2\sqrt{b\pi}}{2c_{22}\left(\gamma_2\eta_2-\gamma_1\eta_1\right)}\left(\frac{1}{2}+\frac{2E(k)}{3F(k)}\right), \tag{65}$$

where

$$p' = \frac{K\left(q_0-q_c\right)}{\lambda\lambda_y b^2}. \tag{66}$$

4. Numerical Results and Discussion

In this section, numerical results are carried out to research the effects of the dimensionless thermal resistance of the cracks surfaces and the geometries of the cracks on the temperature change and the mode II stress intensity factors under the antisymmetrical linear heat flow. A ceramic material of Tyrannohex is chosen and the corresponding material properties are given in [35]. That is, one has

$$E_{xx} = 135.0\,\text{GPa},$$
$$E_{yy} = 87.0\,\text{GPa},$$
$$G_{xy} = 50.0\,\text{GPa},$$
$$v_{xy} = 0.15,$$
$$v_{yx} = 0.09667,$$

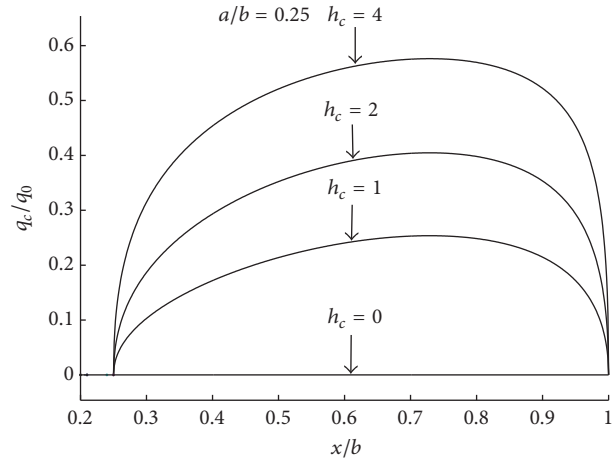

Figure 2: The variations of q_c/q_0 versus x/b with $a/b = 0.25$ and $h_c = 0,\ 1,\ 2,$ and 4, respectively.

$$\alpha_{xx} = 0.32\times10^{-5}/^{\circ}\text{C},$$
$$\alpha_{yy} = 0.32\times10^{-5}/^{\circ}\text{C},$$
$$\lambda_x = 3.08\,\text{W/m}^{\circ}\text{C},$$
$$\lambda_y = 2.81\,\text{W/m}^{\circ}\text{C}. \tag{67}$$

Figure 2 shows the variations of q_c/q_0 versus x/b with $a/b = 0.25$ and $h_c = 0,\ 1,\ 2,$ and 4, respectively. Obviously, when $h_c = 0$, we have $q_c = 0$, corresponding to fully thermally insulated cracks. When $h_c = 1$, it means that if the heat conduction through the cracks region is the same as that of the orthotropic material, the cracks approximate to thermally permeable ones. Moreover, one can find it is feasible to reduce the thermal stress concentrations near the crack-tips by the way of filling the matrix material into a crack in engineering problems. When $h_c = 2$ or $h_c = 4$, it shows the heat conduction through the crack region is twice or 4 times as much as thermal conductivities of an orthotropic material. When $h_c \to \infty$, we have $q_c = q_0$, which means fully thermally permeable cracks. It is revealed that applying the thermally insulated assumption $h_c = 0$ will underestimate much the heat flux to the crack surfaces and applying the fully thermally permeable assumption $h_c \to \infty$ will overestimate much the heat flux to the crack surfaces. The observation reveals that the effects of the heat conduction through the crack region on the crack-tip thermoelastic fields cannot be disregarded.

Figure 3 shows the variations of K/K_0 versus x/b with $h_c = 1$ and $a/b = 0.25,\ 0.5,$ and 0.75, respectively. Figure 4 shows variations of K/K_0 versus x/b with $a/b = 0.25$ and $h_c = 1,\ 2,$ and 4, respectively. Hereafter K_0 stands for the mode II stress intensity factor for a single and fully thermally insulated crack with the length of $2b$ under the antisymmetrical linear heat flow. K/K_0 tends to zero as h_c increases. Obviously, it is unrealistic to assume that the crack is fully thermally permeable. From the above results, it is revealed that the fully

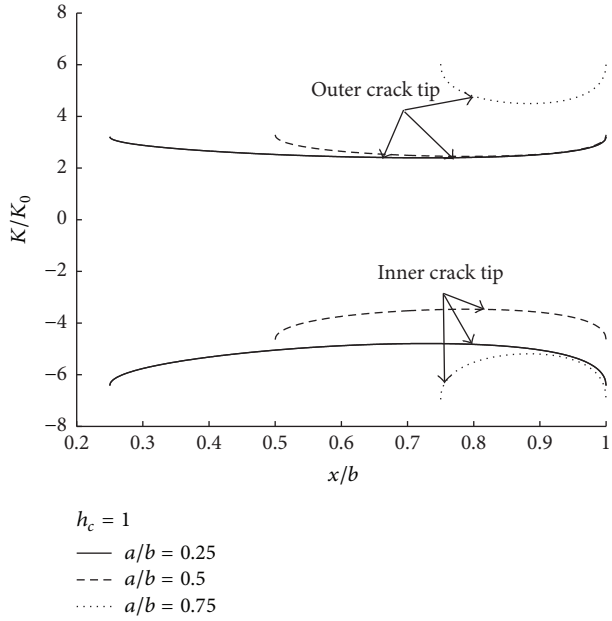

FIGURE 3: The variations of K/K_0 versus x/b with $h_c = 1$ and $a/b = 0.25$, 0.5, and 0.75, respectively.

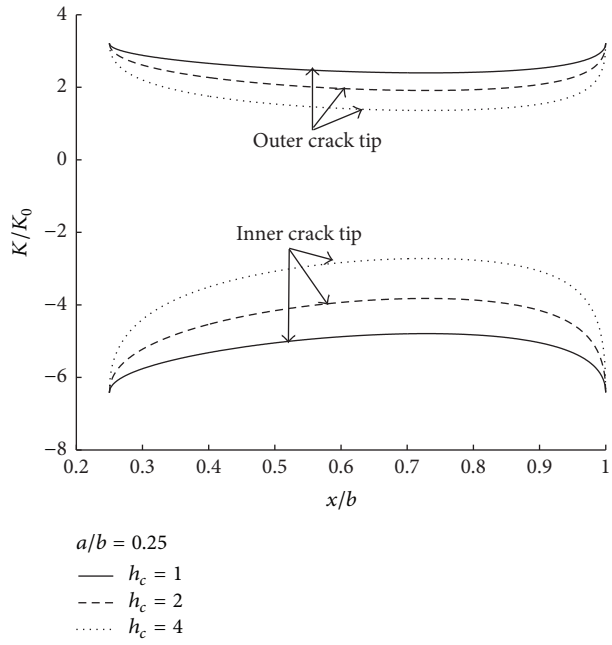

FIGURE 4: The variations of K/K_0 versus x/b with $a/b = 0.25$ and $h_c = 1, 2$, and 4, respectively.

thermally insulated or fully thermally permeable assumption on the crack-face is only a limiting case of a real crack. It is concluded that the material properties and the thermal resistance in the heat conduction through the crack region are of much importance and should be considered in analyzing the thermoelastic problem of a cracked material with a thermal loading. EM solutions for the stress intensity factor K are used to compare with the solutions obtained using the method outlined above.

Figures 6 and 7 present the temperature profile and thermal stress analysis results, respectively. Another model is employed to check the mesh density convergence, with a local mesh four times finer than the mesh used in this analysis. The maximum difference between these meshes is less than 1%. For crack-tip A, the difference between present solution K_{II} and those obtained using FEM is less than 2%. However, the present solution K_{II} for crack-tip B differs from the FEM solutions by up to 20%. Upon examination, the differences in these analyses are due to the assumption of crack being open during the calculation of stress intensity factors. This assumption is not validated by FEM analysis. To overcome this shortcoming, the friction in closed crack surface region should be considered, in order to obtain more accurate values for K_{II} at tip B. As this is beyond the scope of the present paper, it will be a topic to consider for future studies.

5. Conclusions

Considering the effects of the thermal resistance, the problem of two collinear cracks in an orthotropic solid under antisymmetrical linear heat flow is addressed. Applying the Fourier transform technique, the thermoelastic fields involving the jumps of temperature, the elastic displacements across the cracks, and the mode II stress intensity factors are given in closed forms. Numerical results are carried out to show the heat flux to the crack surfaces q_c depends on the geometries of the cracks, the material properties, and applied thermal loading, and the mode II stress intensity factors are dependent on the heat flux to the crack surfaces q_c, the material properties, and the geometries of the cracks. The fully thermally permeable or fully thermally insulated cracks are the limiting case of the partially insulated cracks. The observations reveal that the thermal resistance in the heat conduction through the crack region is of much importance and should not be neglected in analyzing the thermoelastic problem of a cracked material with a thermal loading. Also, FEM solutions for the stress intensity factor K are used to compare with the solutions obtained using the method; it is revealed that the friction in closed crack surface region should be considered. As this is beyond the scope of the present paper, it will be a topic to consider for future studies.

Appendix

To investigate the accuracy of this methodology, FEM solutions for the stress intensity factor K are used to compare with the solutions obtained using the method outlined above. For this problem, an orthotropic plate (thickness = 1 mm) with cracks is considered to be H long and W wide. As shown in Figure 5, the dimensions H, W, $a(a = a')$, and b $(b = b')$ are chosen to be 20 mm, 40 mm, 1 mm, and 4 mm, respectively. The ambient temperature and the heat flux are set at 20.0°C and 400 J, respectively. The resultant mesh has 1,472 elements (using an 8-noded isoparametric

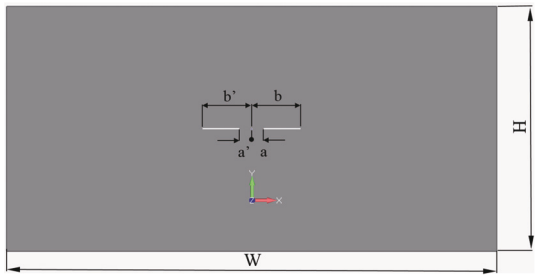

Figure 5: The plate with two collinear cracks is modelled.

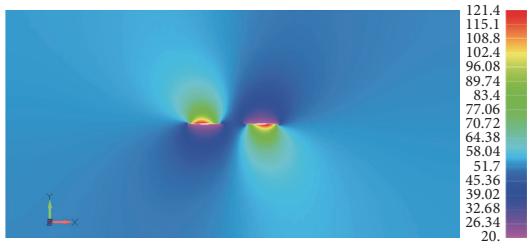

Figure 6: Temperature profile in an orthotropic plate with two collinear cracks under antisymmetrical linear heat flow.

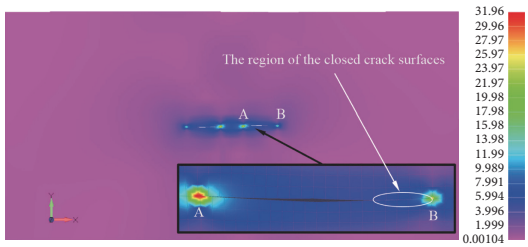

Figure 7: Thermal stress analysis results and crack local detail.

element model) and 4,711 nodes by using software FEMAP [36]. To model the singularity effect we use a fine mesh in the vicinity of the crack-tip region. Gap elements are inserted between crack surfaces to prevent crack top and bottom surface penetrating each other. The "quarter point element" method [37] is used in this section. The midpoint node is moving to the 1/4 point for the elements surrounding the crack-tip. This method uses the displacement field on the crack-face. This has an advantage over the stress correlation method because displacements are primary solution variables in the finite element method and can be obtained with higher degree precision than the stress field. Williams et al. [38] propose an equation to calculate SIF from FEM to include the effect of the crack length on the element size at the crack-tip:

$$K_{\mathrm{I}} = \frac{E_{yy}\delta_y}{8}\sqrt{\frac{2\pi}{l\,(1-l/\,(b-a))}},$$
$$K_{\mathrm{II}} = \frac{E_{xx}\delta_x}{8}\sqrt{\frac{2\pi}{l\,(1-l/\,(b-a))}}, \quad \text{(A.1)}$$

where δ_x and δ_y are the crack opening displacement in y and x direction and l is the distance from the crack-tip. The stress intensity factors obtained using FEM are given as follows:

At crack-tip A, $K_{\mathrm{II}} = 0.974\,\mathrm{Mpa(m)}^{1/2}$ and $K_{\mathrm{I}} = 0.0342\,\mathrm{Mpa(m)}^{1/2}$.

At crack-tip B, $K_{\mathrm{II}} = 0.534\,\mathrm{Mpa(m)}^{1/2}$ and $K_{\mathrm{I}} = 0\,\mathrm{Mpa(m)}^{1/2}$ (as the crack surface near crack-tip B has closed, see Figure 7).

Conflicts of Interest

The authors declare that there are no conflicts of interest regarding the publication of this paper.

Acknowledgments

This work was supported by National Key R&D Program of China (2017YFC0404800), by the Fundamental Research Funds for the Central Universities (no. 2015B35814, no. 2015B41914, and 2017B20614), by the China Scholarship Council (no. 201606710018), and by the National Natural Science Foundation of China (no. 51479052).

References

[1] G. C. Sih, J. Michopoloulos, and S. C. Chou, *Hygrothermoelasticity*, Martinus Niijhoof Publishing, Leiden, The Netherlands, 1986.

[2] G. R. Trwin, "Analysis of stress and strains near the end of a crack transversing a plate," *Journal of Applied Mechanics*, vol. 24, pp. 109–114, 1957.

[3] J. R. Rice, "A path independent integral and the approximate analysis of strain concentration by notches and cracks," *Journal of Applied Mechanics*, vol. 35, no. 2, pp. 379–386, 1968.

[4] J. L. Nowinski, *Theory of Thermoelasticity with Applications*, Sijthoff and Noordhoff, Alphen aan den Rijn, The Netherlands, 1978.

[5] C. Atkinson and D. L. Clements, "On some crack problems in anisotropic thermoelasticity," *International Journal of Solids and Structures*, vol. 13, no. 9, pp. 855–864, 1977.

[6] G. C. Sih, "On the singular character of thermal stresses near a crack tip," *Journal of Applied Mechanics*, vol. 29, no. 3, p. 587, 1962.

[7] Y. M. Tsai, "Orthotropic thermoelastic problem of uniform heat flow disturbed by a central crack," *Journal of Composite Materials*, vol. 18, no. 2, pp. 122–131, 1984.

[8] B. X. Chen and X. Z. Zhang, "Thermoelasticity problem of an orthotropic plate with two collinear cracks," *International Journal of Fracture*, vol. 38, no. 3, pp. 161–192, 1988.

[9] W. K. Wilson and I. W. Yu, "The use of J-integral in thermal stress crack problems," *International Journal of Fracture*, vol. 15, pp. 377–387, 1979.

[10] D. Chang and A. Kotousov, "A strip yield model for two collinear cracks," *Engineering Fracture Mechanics*, vol. 90, pp. 121–128, 2012.

[11] N. N. V. Prasad, M. H. Aliabadi, and D. P. Rooke, "The dual boundary element method for transient thermoelastic crack problems," *International Journal of Solids and Structures*, vol. 33, no. 19, pp. 2695–2718, 1996.

[12] L. M. Brock, "Reflection and diffraction of plane temperature-step waves in orthotropic thermoelastic solids," *Journal of Thermal Stresses*, vol. 33, no. 9, pp. 879–904, 2010.

[13] S. Thangjitham and Choi H. J., "Thermal stress singularities in an anisotropic slab containing a crack," *Mechanics of Materials*, vol. 14, no. 3, pp. 223–238, 1993.

[14] K. Hu and Z. Chen, "Thermoelastic analysis of a partially insulated crack in a strip under thermal impact loading using the hyperbolic heat conduction theory," *International Journal of Engineering Science*, vol. 51, pp. 144–160, 2012.

[15] K. Q. Hu and Z. T. Chen, "Transient heat conduction analysis of a cracked half-plane using dual-phase-lag theory," *International Journal of Heat and Mass Transfer*, vol. 62, no. 1, pp. 445–451, 2013.

[16] X.-C. Zhong and K. Y. Lee, "A thermal-medium crack model," *Mechanics of Materials*, vol. 51, pp. 110–117, 2012.

[17] X.-F. Li and K. Y. Lee, "Effect of heat conduction of penny-shaped crack interior on thermal stress intensity factors," *International Journal of Heat and Mass Transfer*, vol. 91, Article ID 12302, pp. 127–134, 2015.

[18] D. N. Basu, S. Bhattacharyya, and P. K. Das, "Development of a unified model for the steady-state operation of single-phase natural circulation loops," *International Journal of Heat and Mass Transfer*, vol. 62, no. 1, pp. 452–462, 2013.

[19] V. Sundararaman and B. D. Davidson, "An unsymmetric end-notched flexure test for interfacial fracture toughness determination," *Engineering Fracture Mechanics*, vol. 60, no. 3, pp. 361–377, 1998.

[20] S. El-Borgi, F. Erdogan, and L. Hidri, "A partially insulated embedded crack in an infinite functionally graded medium under thermo-mechanical loading," *International Journal of Engineering Science*, vol. 42, no. 3-4, pp. 371–393, 2004.

[21] M. Rekik, S. El-Borgi, and Z. Ounaies, "The axisymmetric problem of a partially insulated mixed-mode crack embedded in a functionally graded pyro magneto-electro-elastic infinite medium subjected to thermal loading," *Journal of Thermal Stresses*, vol. 35, no. 11, pp. 947–975, 2012.

[22] M. Rekik, M. Neifar, and S. El-Borgi, "An axisymmetric problem of a partially insulated crack embedded in a graded layer bonded to a homogeneous half-space under thermal loading," *Journal of Thermal Stresses*, vol. 34, no. 3, pp. 201–227, 2011.

[23] N. I. Mushkelishvili, *Singular Integral Equations*, Wolters-Noorhoff, Groningen, The Netherlands, 1953.

[24] F. Cakoni and D. Colton, "The linear sampling method for cracks," *Inverse Problems*, vol. 19, no. 2, pp. 279–295, 2003.

[25] Q. H. Qin, *The Trefftz Finite and Boundary Element Method*, WIT Press, Southampton, UK, 2000.

[26] A.-Y. Kuo, "Effects of crack surface heat conductance on stress intensity factors," *Journal of Applied Mechanics*, vol. 57, no. 2, pp. 354–358, 1990.

[27] K. Y. Lee and S.-J. Park, "Thermal stress intensity factors for partially insulated interface crack under uniform heat flow," *Engineering Fracture Mechanics*, vol. 50, no. 4, pp. 475–482, 1995.

[28] Y.-D. Lee and F. Erdogan, "Interface cracking of FGM coatings under steady-state heat flow," *Engineering Fracture Mechanics*, vol. 59, no. 3, pp. 361–380, 1998.

[29] Y. Zhou, X. Li, and D. Yu, "A partially insulated interface crack between a graded orthotropic coating and a homogeneous orthotropic substrate under heat flux supply," *International Journal of Solids and Structures*, vol. 47, no. 6, pp. 768–778, 2010.

[30] Y. T. Zhou and K. Y. Lee, "Thermal response of a partially insulated interface crack in a graded coating-substrate structure under thermo-mechanical disturbance: Energy release and density," *Theoretical and Applied Fracture Mechanics*, vol. 56, no. 1, pp. 22–33, 2011.

[31] N. A. Weiss and L. M. Keer, "Heat flow disturbed by periodic array of insulated interface cracks," *Mechanics Research Communications*, vol. 54, pp. 50–55, 2013.

[32] Y.-T. Zhou and T.-W. Kim, "Thermal resistance inside an interface crack in the functionally graded sandwich structures," *Fatigue and Fracture of Engineering Materials and Structures*, vol. 39, no. 9, pp. 1067–1080, 2016.

[33] I. S. Gradshteyn and I. M. Ryzhik, *Table of Integrals, Series, and Products*, Elsevier Academic Press, San Diego, Calif, USA, 2007.

[34] X.-C. Zhong, "Closed-form solutions for two collinear dielectric cracks in a magnetoelectroelastic solid," *Applied Mathematical Modelling*, vol. 35, no. 6, pp. 2930–2944, 2011.

[35] S. Itou, "Thermal stress intensity factors of an infinite orthotropic layer with a crack," *International Journal of Fracture*, vol. 103, no. 3, pp. 279–291, 2000.

[36] *FEMAP—Finite Element Modelling and Post Processing Version 11.1.2*, Structural Dynamics Research Corporation, Pennsylvania, 2015.

[37] R. Barsoum, "Further application of quadratic isoparametric elements to linear fracture mechanics of plate bending and general shells," *International Journal of Numerical Methods Engineering*, vol. 11, pp. 167–169.

[38] J. F. Williams, R. Jones, and N. Goldsmith, "An introduction to fracture mechanics theory and case studies," *Transactions of the Institution of Engineers, Australia Mechanical Engineering*, vol. 44, pp. 185–223, 1989.